

2018

## Investigation of Wavenumber Calibration for Raman Spectroscopy Using a Polymer Reference

Dongyue Liu

*National University of Ireland, Maynooth*

Hugh Byrne

*Technological University Dublin, hugh.byrne@tudublin.ie*

Luke O'Neill

*Technological University Dublin, Luke.oneill@tudublin.ie*

Bryan M. Hennelly

*National University of Ireland, Maynooth*

Follow this and additional works at: <https://arrow.tudublin.ie/radcon>



Part of the [Optometry Commons](#), and the [Physical Sciences and Mathematics Commons](#)

---

### Recommended Citation

Liu, D., Byrne, H. & O'Neill, L. (2018). Investigation of Wavenumber Calibration for Raman Spectroscopy Using a Polymer Reference. *Proceedings of SPIE - The International Society for Optical Engineering*, vol.10680, no. 1068027, SPIE Photonics Europe 2018, 22-26 April 2018Strasbourg Convention & Exhibition Centre/Strasbourg, France. 10.1117/12.2307574

This Conference Paper is brought to you for free and open access by the Radiation and Environmental Science Centre at ARROW@TU Dublin. It has been accepted for inclusion in Conference papers by an authorized administrator of ARROW@TU Dublin. For more information, please contact [yvonne.desmond@tudublin.ie](mailto:yvonne.desmond@tudublin.ie), [arrow.admin@tudublin.ie](mailto:arrow.admin@tudublin.ie), [brian.widdis@tudublin.ie](mailto:brian.widdis@tudublin.ie).



This work is licensed under a [Creative Commons Attribution-NonCommercial-Share Alike 3.0 License](#)

# Investigation of wavenumber calibration for Raman spectroscopy using a polymer reference

Dongyue Liu<sup>a</sup>, Hugh J. Byrne<sup>b</sup>, Luke O'Neill<sup>b</sup>, Bryan Hennelly<sup>\*a,c</sup>

<sup>a</sup>Department of Electronic Engineering, Maynooth University, Co. Kildare, Ireland

<sup>b</sup>FOCAS Research Institute, Dublin Institute of Technology, Kevin Street, Dublin 8, Ireland

<sup>c</sup>Department of Computer Science, Maynooth University, Co. Kildare, Ireland

## ABSTRACT

Raman spectroscopy is an optical technique that can be used to evaluate the biomolecular composition of tissue and cell samples in a real-time and non-invasive manner. Subtle differences between datasets of spectra obtained from related cell groups can be identified using multivariate statistical algorithms. Such techniques are highly sensitive to small errors, however, and, therefore, the classification sensitivity of Raman spectroscopy can be significantly impacted by miscalibration of the optical system due to small misalignments of the optical elements and/or variation in ambient temperature. Wavenumber calibration is often achieved by recording the spectrum from a wavenumber reference standard, such as 4-acetamidophenol or benzene, which contains numerous sharp peaks in the fingerprint region. Here, we investigate a commercial polymer slide as a wavenumber reference standard for the calibration of Raman spectra. The Raman spectrum of this slide contains numerous sharp peaks in the fingerprint region. Unlike many other reference standards, the polymer slide is non-hazardous, has an indefinite lifetime, and is designed in the shape of a glass slide used for microscopy. We evaluate this reference in terms of accuracy and repeatability, and we compare with the established 4-Acetamidophenol wavenumber reference.

**Keywords:** Raman spectroscopy, wavenumber calibration, peak stability, wavenumber reference, 4-Acetamidophenol.

## 1. INTRODUCTION

Raman spectroscopy is based on the inelastic scattering of monochromatic light.<sup>1</sup> The phenomenon was first discovered by Sir C. V. Raman, for which he won the 1930 Nobel Prize in physics. Recent technological developments have made Raman spectroscopy an affordable, non-destructive, and reliable analytical technique. It is possible to identify a specific substance by inspecting the Raman spectrum that is recorded from that substance. For this reason, Raman spectra are sometimes referred to as fingerprints. Raman spectroscopy is utilized in many fields, such as chemistry, physics, biology and medical science.<sup>1-7</sup> Raman spectroscopy has many advantages over other similar methods, including fast detection-speed, repeatability, the requirement for low sample volumes, as well as being non-destructive. Traditionally, Raman systems have been laboratory-based; however, the footprint and cost of optical Raman spectroscopy systems have significantly reduced in recent years; in aviation security for example, spatially offset Raman spectroscopy is now used to rapidly identify material within bottles using a database of spectra recorded from various substances.<sup>2</sup>

An application of Raman spectroscopy that is receiving significant attention is the classification of different cell and tissue types, which produce subtly different Raman spectra, due to, for example the presence of disease.<sup>4-7</sup> This involves the training of a statistical algorithm based on known pathological samples. Techniques such as principal component analysis (PCA) and linear discriminant analysis (LDA) are typically employed for the classification of spectra.<sup>4,5</sup> For example, healthy bladder epithelial cells can be distinguished from low-grade and high-grade bladder cancer cells with greater accuracy using Raman spectroscopy than using traditional techniques for cytology and pathology.<sup>8-10</sup> Similarly, Raman spectroscopy combined with multivariate statistical analysis can be used as a diagnostic tool to detect biochemical changes accompanying cervical cancer<sup>11</sup> as well as oral cancer progression.<sup>12</sup> Raman spectroscopy has the additional advantage of providing rapid minimally invasive detection of the disease, which can be fully exploited using fiber optic probes that facilitate endoscopic classification of tissue, or identification of tumour margins in-vivo.<sup>13,14</sup>

\*bryanh@cs.nuim.ie; phone 1 708 3338; fax 1 708 6027

In order to ensure the accuracy of the collected spectrum, and therefore the accuracy of the resultant classification that is based on this spectrum, for any of the applications that have been discussed above, it is of paramount importance to calibrate the instrument. Unfortunately, there exist many sources of error; a small misalignment in the optical system can result in a significant miscalibration, which can, in turn, lead to incorrect classification of the sample. It is, therefore, necessary to perform an accurate calibration procedure before starting to recording data, and it is often necessary to repeat this calibration step routinely throughout a given experiment; it may be expected that over time, even a well-calibrated system will deviate from its initial specification; even normal handling can adversely affect calibration. Optical components such as grating, mirrors, lenses and focusing mirror may move slightly over time resulting in miscalibration. In addition, since Raman scattering is a temperature dependent process, it may be expected that variation in ambient temperature will also affect calibration of the recorded spectrum.<sup>1</sup>

Another point of note is that no two Raman instruments will produce the same raw spectrum for the same sample unless full calibration is performed on both systems, and this has hindered progress in many applications including disease diagnostics. Many companies that build Raman spectrometers implement their own internal methods to control the performance and the stability of their own instruments; however, there is no universally accepted method to control the performance and stability of different instruments. The difficulty in comparing spectra that have been recorded across different instruments is one of the main obstacles in the development of Raman spectroscopy for many applications and to its clinical acceptance, and in recent years a number of different protocols have been proposed to address this key issue.<sup>16-20</sup> Intensity calibration and wavenumber calibration are the main subjects of these protocols. This paper is concerned only with wavenumber calibration.

A number of solutions that perform wavenumber calibration already exist.<sup>21</sup> One solution uses two steps: (i) a known spectrum from a Neon lamp (or similar) allows wavelength calibration of the spectrometer to be performed,<sup>16</sup> followed by (ii) subsequent wavenumber calibration, which is performed using a known standard such as silicon, which produces a well-known sharp peak at  $520\text{ cm}^{-1}$ . A second solution, which uses a single step, is to employ a wavenumber reference standard such as indene,<sup>22,23</sup> cyclohexane,<sup>24-26</sup> benzene,<sup>27</sup> and benzonitrile.<sup>28</sup> These standards contain numerous sharp peaks in their Raman spectra at well-known wavenumber location. A polynomial function can be fitted to these peak positions in order to calibrate the entire wavenumber axis. Often, many wavenumber standards are used at the same time in order to increase the range of, and improve the accuracy of, the calibration.

All of the chemical standards that we reviewed in the literature are hazardous to human health and must be handled in a controlled manner. In this paper, we propose a new wavenumber reference in the form of a commercial polymer slide that is designed for life science applications, which is inexpensive, safe to handle, and chemically stable over time. In Section 2, the various sources of error in a Raman spectrometer are discussed and, in Section 3, the traditional approach of wavenumber calibration using a wavenumber reference is reviewed, specifically for the case of 4-Acetamidophenol, a commonly used wavenumber reference. In Section 4, the peak positions of the polymer are measured and the stability of these peak positions is compared with that of 4-Acetamidophenol. In Section 5, a brief conclusion is offered.

## 2. SOURCES OF ERRORS

There are many sources of error that can lead to miscalibration of a Raman spectrum. Slight rotation of the spectrograph diffraction grating or the CCD (for the case of the CCD we mean in-plane rotation), small lateral displacement of the CCD and small changes in the laser excitation wavelength due to variation in temperature or current will all result in errors in terms of wavenumber position of spectral peaks. The most potent source of error in many Raman systems is the grating angle. Many spectrographs allow for rotation of the grating in order to allow for recording different regions of the spectrum. However, frequent rotation of the motor can lead to error. The best way to correct for this error is to routinely perform a rigorous calibration procedure. In this section, we examine these various sources of error and attempt to relate instrument error to error in the wavenumber axis in the recorded spectrum.

A common feature in a modern spectrograph is the variable rotation of the grating in order to vary the wavenumber band that is recorded on the CCD camera; this is usually achieved using a stepper motor. However, no motor can provide precise repeatability in terms of the rotation angle. As a result, it is difficult to ensure that the expected angle is obtained. The figure below illustrates the effect of an error in the angle of 0.1 degrees in terms of the resulting error in both wavelength, see Fig.1 (a), and in wavenumber, which is shown in Fig. 1 (b). This calculation is based on the grating equation and the optical configuration of a Czerny-Turner spectrograph such as that used in the experimental system

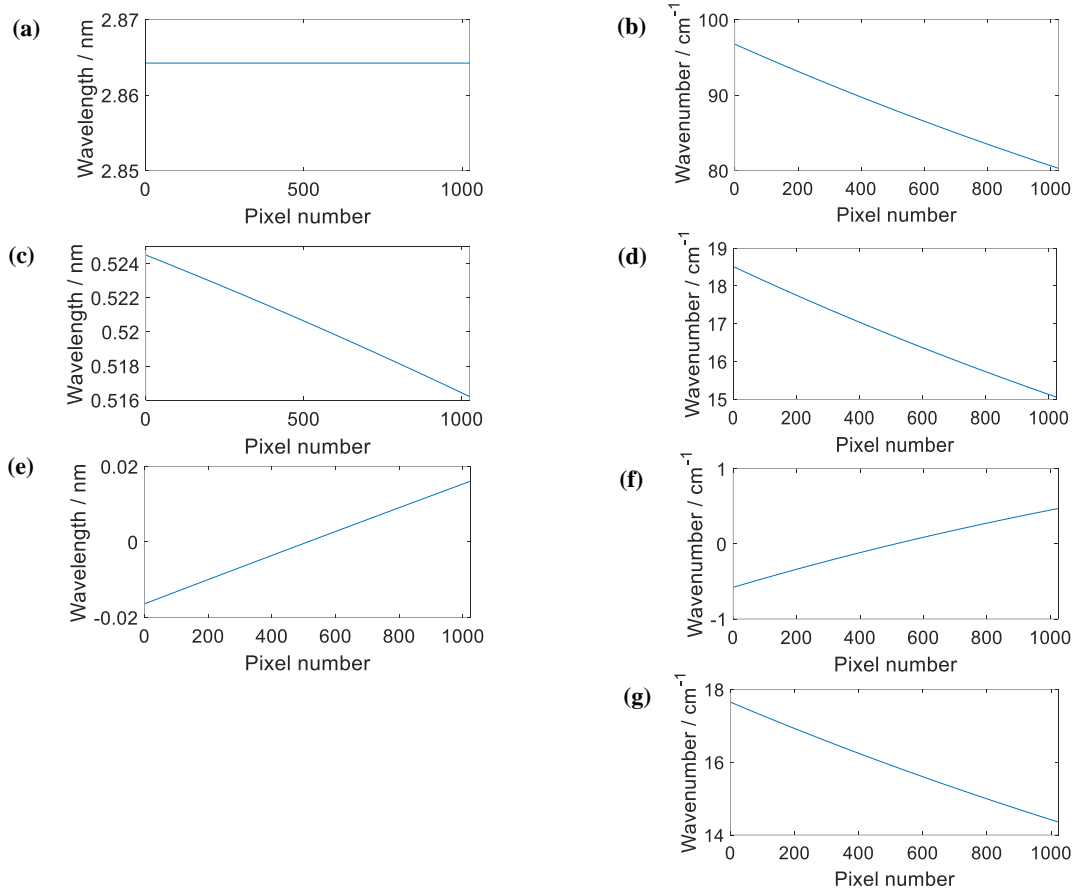


**Figure 1.** (a) shows the wavelength error caused by the 0.1-degree rotation in the grating as a function of pixel number and (b) shows the corresponding error in wavenumber; (c) shows the error in the wavelength axis as a function of pixel number, caused by a lateral displacement of the camera by an amount equal to the width of 10 pixels (approximately 0.25mm) and (d) shows the corresponding error in wavenumber; (e) shows the error in wavelength as function of pixel number caused by an in-plane rotation of the camera sensor by an angle of  $2^\circ$  and (f) shows the corresponding error in wavenumber. Finally (g) shows the error in wavenumber caused by a shift in the source laser wavelength from an expected value of 532 nm to a value of 532.1nm

described in Section 3. The parameters used in this calculation are the same as similar to those found in the experimental system: source wavelength is 532nm, spectrograph focal length is 0.8m, CCD pixel size is  $26\mu\text{m}$ , and grating incidence angle is  $\theta_1 = 11^\circ$  and groove density of the grating is 600 lines/mm. Fig. 1 (a) shows the error in wavelength that occurs when an expected angle of  $11^\circ$  is used to calculate the wavelength axis for the spectrum, and the actual grating angle is  $11.1^\circ$ ; the resulting error in the wavelength axis is approximately 2.83nm for all pixels. In Fig. 1 (b) the corresponding error is shown for the wavenumber axis; this error varies from  $100\text{ cm}^{-1}$  to  $80\text{ cm}^{-1}$  across the spectrum.

The second source of error that is considered here is unexpected displacement of the camera, which may occur if the camera is replaced. The error in both the wavelength and wavenumber positions of spectral peaks resulting from a shift of 0.26 mm (10 pixels) is shown in Fig. 1 (c) and Fig. 1 (d), respectively for the same parameters used in the previous example. In Fig. 1 (c) it can clearly be seen that shift 10 camera pixels will result in approximately 0.5nm error for every point in the spectrum; more accurately, the error varies from 0.515nm to 0.525nm across the spectrum. Similarly, in Fig. 2 (d) it can be seen that in terms of wavenumber, this corresponds to an error of between  $15\text{ cm}^{-1}$  and  $18.5\text{ cm}^{-1}$  across the face of the camera. It can be concluded that a small shift of the camera position results in a significant miscalibration of the wavenumber position of spectral peaks and may lead to significant errors in terms of multivariate classification. Another camera related source of error that may occur is a small unexpected in-plane rotation, which may occur due to the slight incorrect placement of the camera in the output port of the spectrograph as illustrated in Figure 2. This will reduce the effective width of the CCD pixels relative to the plane of the diffraction grating.

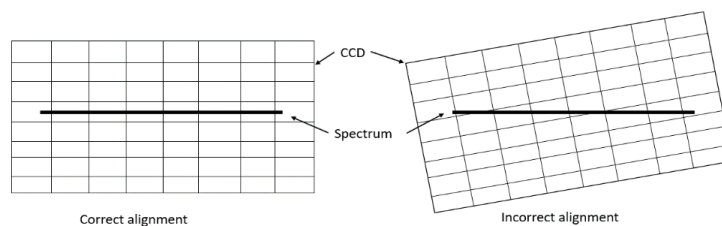


**Fig. 2. Illustration of the error caused by incorrect placement of the CCD camera in terms of in-plane rotation. The angle of rotation shown in the figure is exaggerated.**

If the CCD camera is rotated around its center, the wavelength/wavenumber error at the center pixel number should be zero and will increase at increasing distances from this point. In Fig. 1 (e) the error in wavelength is shown as a function of pixel number for an incorrect placement angle of  $2^\circ$ . The error is zero for the centre pixel but increases to  $\pm 0.02\text{nm}$  at the ends of the camera. The corresponding error in wavenumber is shown in Fig. 1 (f); once again, the error is zero for the centre pixel but increases to  $\pm 0.5\text{cm}^{-1}$  at extreme ends of the camera. Although this is not as potent a source of error as grating rotation or lateral camera displacement, it is, nevertheless, appreciable.

When calculating the wavenumber axis using an already available wavelength axis, the laser wavelength is a key factor. A slight error of laser wavelength can lead to the large difference in the resulting wavenumber axis. Modern solid stable lasers are controlled using highly stabilized laser drivers, which guarantee that a single longitudinal mode is produced; however, the wavelength may vary slightly over long periods of time. In Fig. 1 (g) the resulting error in wavenumber is shown when an expected laser wavelength of  $532\text{nm}$  was used to calculate the wavenumber axis, but the actual laser wavelength is  $532.1\text{nm}$ ; the resulting error varies from  $14\text{cm}^{-1}$  to  $18\text{cm}^{-1}$  across the spectrum. Even a small change in wavelength of  $0.001\text{nm}$  during an experiment will lead to appreciable changes in the wavenumber axis; to overcome this problem, many of the lasers used for Raman spectroscopy have picometer wavelength stability over a number of hours.

The process of Raman scattering is dependent on temperature.<sup>1</sup> Significant changes in temperature can lead to fundamental changes in molecular structure.<sup>1</sup> A change in temperature can, therefore, change a Raman spectrum in ways that are sample dependent; peak broadening can occur, as can changes in peak intensity; however, such changes are not typically reported for the types of samples used in the applications discussed in Section 1, over the range of normal ambient temperatures that can be expected in a laboratory environment. However, changing temperature may also result in miscalibration of the wavenumber axis by a few wavenumbers, which may be due to slight thermal expansion of the optical elements. The problem can be mitigated by controlling room temperature. It is not straightforward to simulate an error in wavenumber due to temperature change; instead, an experiment was designed to investigate this effect. A polymer slide, discussed in more detail in Section 3, was illuminated by a  $532\text{nm}$  wavelength laser source using the experimental set-up described below, with no temperature control. The position of one peak was measured for 1000 consecutive 10s acquisitions. The wavenumber position of this peak as a function of the sequence number is shown in Fig. 3; an increase in the mean wavenumber position of almost  $2\text{cm}^{-1}$  is measured from the beginning of the experiment to the end; ambient temperature was recorded to have increased by approximately  $3^\circ\text{C}$  during this time. We note that this effect may be the result of other sources of error; a more controlled experiment would be required to conclusively relate temperature change to instrument miscalibration.

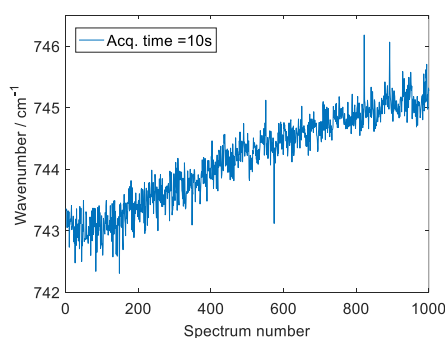


**Fig. 3. Change in wavenumber position a spectral peak for a polymer sample over time.**

### 3. WAVENUMBER CALIBRATION USING A WAVENUMBER REFERENCE

The purpose of this section is two-fold. Firstly, the protocol used for wavenumber calibration using a wavenumber reference is described in detail and experimental results are shown describing each step using a sample of 4-Acetamidophenol, a commonly used wavenumber reference standard. Secondly, the newly calibrated instrument is used to record the (calibrated) spectrum from a commercial polymer slide that is commonly used for life science purposes ( $\mu$ -Slide I Luer, Ibidi GmbH, Munich, Germany).<sup>29</sup> This slide is designed with a flow channel for imaging adherent cells under flow conditions as well as 3D cell culture. The base of the slide is made of a transparent polymer with coverslip thickness to facilitate imaging with an inverted microscope. The properties of autofluorescence, birefringence, and the refractive index of the Ibidi polymer coverslip are similar to those of glass, allowing for the use of all kinds of objective lenses including oil immersion; the specific chemical structure of the polymer material is proprietary, and could not be ascertained for this paper. In Section 4, we explore the potential of this polymer slide to be used as a wavenumber reference by analysing the stability of the peaks in the polymers Raman spectrum and comparing these results to those obtained from 4-Acetamidophenol.

The protocol for using a wavenumber reference to perform wavenumber calibration has been developed in many other references<sup>16-20</sup>. The steps involve:

- (i) Recording the spectrum from a sample with a pure chemical that has a known Raman spectrum containing a number of sharp peaks at well-defined wavenumber positions.
- (ii) Obtaining the precise wavenumber positions from a reliable source such as the American Society for Testing Materials (ASTM) or the National Institute of Standards and Technology.
- (iii) Recording the sample (pixel) position of each of these peaks in the spectrum, and pairing these with their respective wavenumber positions to provide a set of two-dimensional coordinates in the form (pixel, wavenumber).
- (iv) Applying a polynomial fit to these coordinates using the method of classical least squares. The resulting polynomial provides the relationship between every pixel and the corresponding wavenumber.

Further detail on these steps can be found in Ref [16]. The number of peaks that are needed to perform accurate calibration has been a subject of interest in the literature, as has the order of the polynomial that should be used in the Step (iv).<sup>16-20</sup> The accuracy can be shown to be dependent on the number and position the peaks and a large number of peaks covering as wide an area of the spectrum should be used. In order to increase the number and range of peaks used in the calibration, some researchers have used multiple chemical references in a single calibration.<sup>16</sup> The order of the polynomial should not be so large as to result in overfitting but not so small to result in under fitting; a polynomial order of four has been shown to perform well.<sup>16</sup> The pixel positions that are recorded in Step (iii) can be obtained with sub-pixel accuracy using a process of interpolation as proposed in Ref. [16]. In the experiment that follows, we perform cubic-spline interpolation in the area of each peak in order to accurately identify the position of each peak.

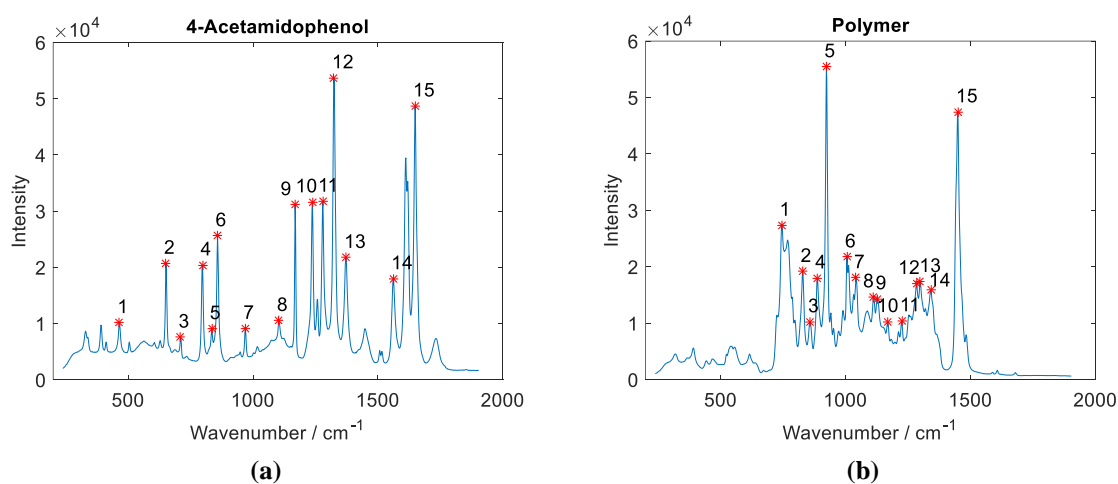


**Fig. 4. (a) Raman spectrum of the 4-Acetamidophenol spectrum. (b) Raman spectrum of the polymer sample. For both cases, the wavenumber axis has been calibrated using the calibration protocol described in this section, applied to the peaks positions of the 4-Acetamidophenol spectrum**

Spectra were recorded using a custom built confocal Raman microspectrometer operating with a 532nm laser (150mW, Torus; Laser Quantum, Cheshire, UK), 10x microscope objective (10 / 0.3 Olympus MPlanFl; Olympus Corporation, Japan), and 100 $\mu$ m confocal aperture. Raman scattered photons are collected with a spectrograph (Shamrock 500; Andor Technology, UK) operating with a 1000 lines/mm grating (spectral resolution of 2.5cm<sup>-1</sup> at the centre), and a cooled CCD camera (Newton 920; Andor Technology, UK) operating at -80°C. More details on this optical system are available in Ref. [9]. The chemical used to calibrate our instrument is 4-Acetamidophenol, a commonly used wavenumber reference standard. A pure sample of this chemical was obtained from a commercial source (Sigma Aldrich, Wicklow, Ireland) and the wavenumber positions of the peaks were obtained from an international standards organisation (ASTM International, Pennsylvania, US), which are shown below in Table 1.

Peak number	4-Acetamidophenol Reference (cm <sup>-1</sup> )	Polymer Spectrum (cm <sup>-1</sup> )
1	465.1	743.5267
2	651.6	827.9567
3	710.8	857.9544
4	797.2	886.563
5	834.5	923.0671
6	857.9	1005.7366
7	968.7	1041.7295
8	1105.5	1111.6935
9	1168.5	1127.9242
10	1236.8	1168.3634
11	1278.5	1224.6504
12	1323.9	1283.9253
13	1371.5	1297.9906
14	1561.6	1340.9552
15	1648.4	1449.3456

**Table 1 The reference table of spectral peak positions for a sample of 4-Acetamidophenol (ASTM E1840-96) and the (calibrated) spectral peak positions of the polymer sample.**

Five spectra, each with an acquisition time of 16s, were recorded from 4-Acetamidophenol sample, contained in a vial with a base made from a Raman grade Calcium Fluoride (Crystran, UK) coverslip with a thickness of 200 $\mu$ m. This acquisition time was just less than that which would cause saturation of the camera. These five spectra were averaged to produce a low noise Raman spectrum with a total acquisition time of 80s, which completes Step (i). This average spectrum is shown in Fig. 4 (a). The sharpest 15 peaks were selected for use in the calibration process and these are numbered from 1-15 in the figure. The wavenumber position of each of these peaks was obtained from Table 1, completing Step (ii). In Fig. 5 (a), the fifteen coordinates that result from Step (iii) as well as the fourth order polynomial that was fitted to these coordinates in Step (iv) are both shown. The positions of the peaks is determined with sub-pixel accuracy using cubic spline interpolation.<sup>29</sup> The third order polynomial that is associated with each of the fifteen peaks is isolated and the derivative of this function provides a solution for an accurate (sub-pixel) position of each peak. This process is illustrated in Fig. 5 (b). These values of the pixel position of the peaks are used to define the coordinates used for polynomial fitting, shown in Fig. 5 (a). The calibrated wavenumber axis, which is obtained by relating each pixel position to its corresponding wavenumber value using this polynomial function, is shown in Fig. 4 (a).

Immediately following calibration of the system, as described above, five spectra, each with an acquisition time of 16s, were recorded from the polymer slide. In this case no sample container was necessary; the slide has the same dimensions as a traditional glass slide used in microscopy (7cm  $\times$  2.5cm  $\times$  1mm), and can be easily placed on a microscope translation stage. Once again, these five spectra were averaged to produce a low noise Raman spectrum with a total acquisition time of 80s.

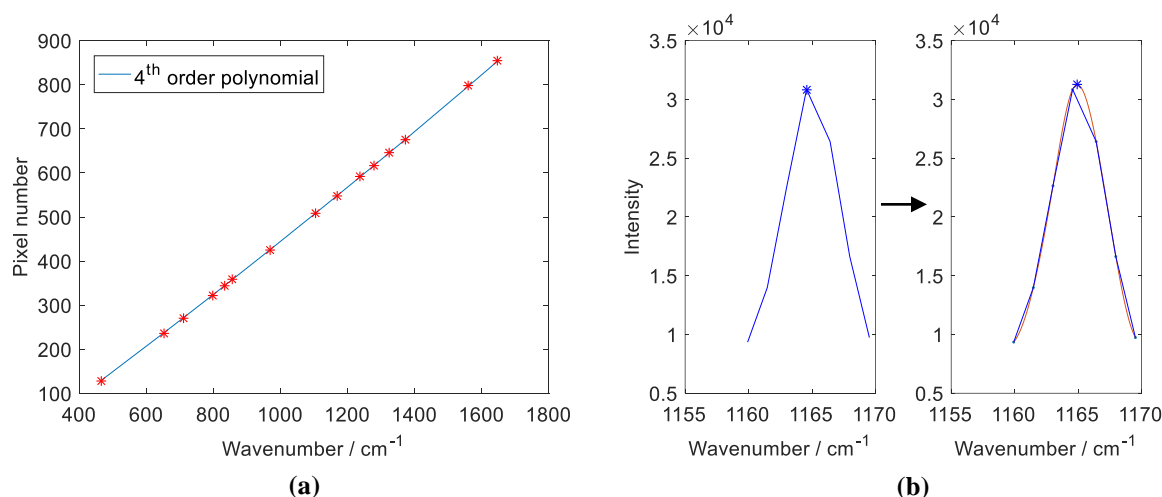


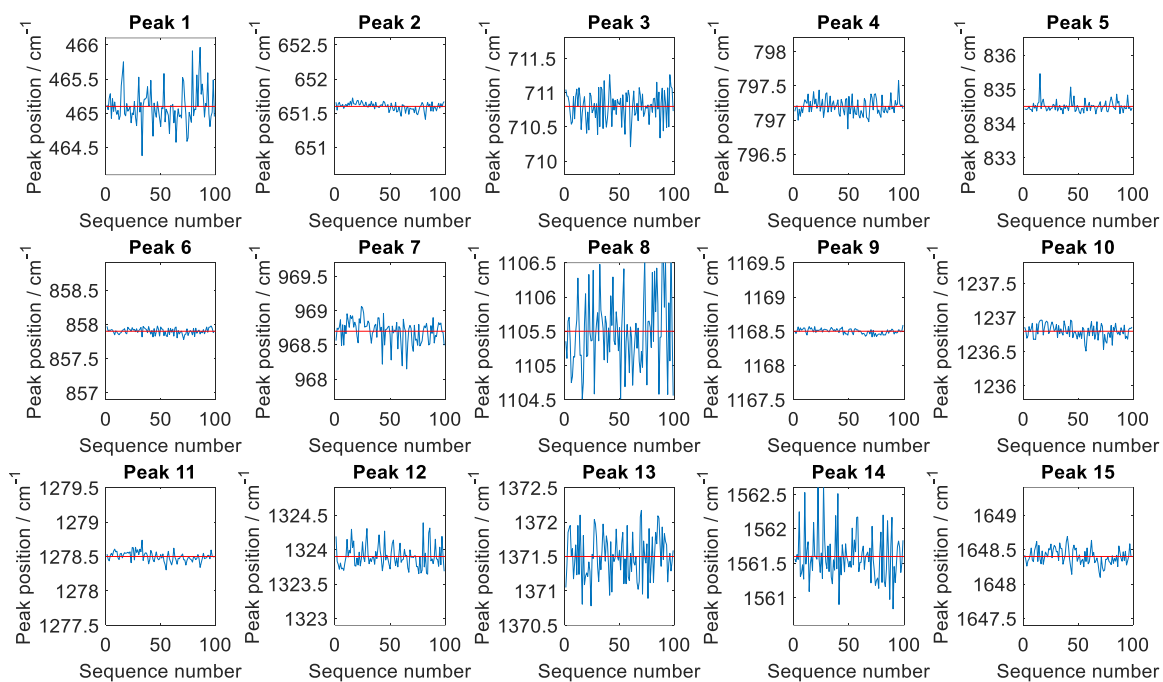
**Fig. 5. (a) Plot of the fifteen coordinates obtained by Step (iii) of the calibration protocol using 4-Acetamidophenol, as well as the polynomial fit from Step (iv); (b) Illustration of the interpolation process used to obtain sub-pixel accuracy for one peak position. The blue asterisk indicates the peak position with and without interpolation.**

The fifteen sharpest peaks were selected for further inspection, and once again a process of cubic spline interpolation was used to identify the position of the peaks with sub pixel accuracy. The positions were then related to their corresponding wavenumbers using the polynomial function returned from the calibration process already described. The wavenumber position of each of the fifteen peaks is also shown in Table 1. Interestingly, the spectral intensity of the polymer is approximately the same as that from the 4-Acetamidophenol for the same acquisition time, indicating that, if this sample were to be used as a reference, similar acquisition times could be used. In terms of its applicability as a wavenumber reference, it can be seen that the polymer spectrum contains a large number of sharp peaks, albeit over a smaller range of the wavenumber axis. In Section 4, these peaks are investigated further; specifically, we investigate the stability of the peaks positions across different sets of measurements.

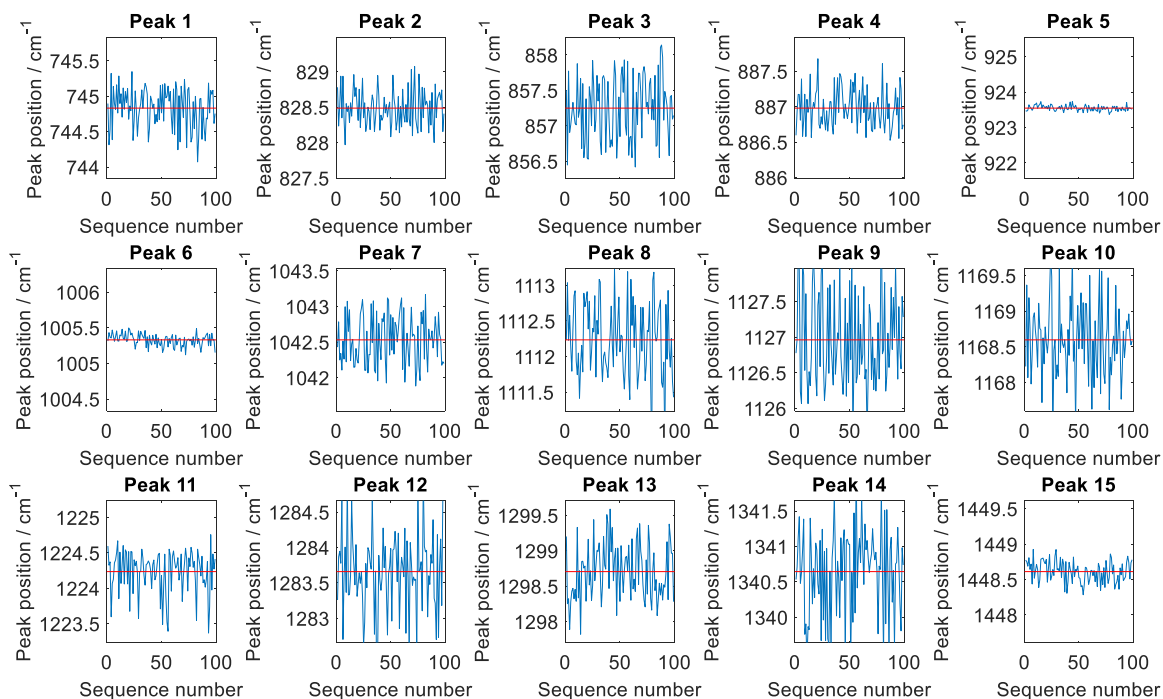
#### 4. EVALUATION OF POLYMER WAVENUMBER REFERENCE

In order to evaluate the potential for the polymer slide to be used a wavenumber reference standard, it is necessary to investigate the stability of the various peaks in terms of wavenumber position. With any peak measurement in Raman spectroscopy, there can be expected small deviation in the position of that peak across a set of measurements. The reason for the instability in peak position is due to the presence of noise, which can affect attempts to accurately measure a peak position. The noise in a Raman spectrum is primarily comprised of shot noise, dark current, read noise<sup>30</sup>; the latter two noise sources originate from the camera but are insignificant compared to the shot noise generated by the types of samples used as wavenumber references. Shot noise is a time-dependent noise contribution that originates from the signal itself. Shot noise<sup>30</sup> is the name given to inconsistent levels of irradiance that are incident on a pixel over a given time,  $t$ . Irradiance per pixel,  $i$ , is typically modeled as a Poisson distribution. The signal to noise ratio (SNR) is given by  $it/(it)^{0.5}$ , which is the signal intensity divided by the standard deviation of the shot noise. It is clear that the SNR increases as a function of the square root of the acquisition time. It is, therefore, important to use a sufficiently long exposure time when recording a reference spectrum. The sharpness of the peak is also a consideration, since an estimation of peak position using the interpolation approach outlined in the previous section will make use of neighboring samples and will, therefore, include their noise contributions in the estimation.

An experiment was conducted to measure the wavenumber stability of the fifteen 4-Acetamidophenol peaks listed in Table 1 as well as for the fifteen polymer peaks. The position of each peak was measured across 100 consecutive recordings, for acquisitions times of 1s, 2s, and 4s. The position of each peak across the sequence of recordings is shown in Fig. 6 (a) for 4-Acetamidophenol and in Fig. 6 (b) for the polymer slide.



(a)



(b)

**Fig. 6** (a) The peak position of the fifteen peaks of 4-Acetamidophenol that are listed in Table 1 for a sequence of 100 spectra with 4s acquisition time. The red line indicates the mean position of the peak. In all cases the vertical axis has a range of  $2\text{cm}^{-1}$ ; (b) The peak position of the fifteen peaks of the polymer slide that are listed in Table 1, also for a sequence of 100 spectra with 4s acquisition time. The red line indicates the mean position of the peak. In all cases the vertical axis has a range of  $2\text{cm}^{-1}$

Peak number	Standard deviation of peak positions for 4-Acetamidophenol			Standard deviation of peak positions for polymer slide		
	1 second	2 seconds	4 seconds	1 second	2 seconds	4 seconds
1	0.6360	0.5704	0.2653	0.5992	0.3988	0.2830
2	0.3745	0.0718	0.0562	0.5073	0.3221	0.2523
3	0.4220	0.3405	0.2207	0.9880	0.6128	0.4502
4	0.3980	0.1755	0.1203	0.5190	0.3971	0.2721
5	0.5891	0.3302	0.1653	0.1481	0.1100	0.0769
6	0.2525	0.0731	0.0447	0.2056	0.1170	0.0845
7	0.4598	0.3417	0.1719	0.6429	0.5208	0.3420
8	0.9100	0.7974	0.5333	1.0037	0.6943	0.5167
9	0.2918	0.0507	0.0374	1.2029	0.7591	0.6542
10	0.2961	0.1478	0.0983	1.0578	0.6561	0.5158
11	0.3817	0.1080	0.0694	0.5709	0.4253	0.3002
12	0.4064	0.2349	0.1665	0.8866	0.6989	0.5604
13	0.6736	0.4030	0.3238	0.7638	0.6362	0.3891
14	0.6036	0.4034	0.3475	0.9761	0.8536	0.6106
15	0.3693	0.1708	0.1154	0.2701	0.1751	0.1502
Mean	0.4710	0.2813	0.1824	0.6895	0.4918	0.3639

Table 2 shows the standard deviation of the wavenumber position of each peak for both samples for four different acquisition times. The values for the '4 sec' columns are standard deviation of the functions shown in Fig. 6.

A comparison of the peaks that appear in the spectrum of 4-Acetamidophenol, shown in Fig. 4 (a), with the variation in the corresponding peak positions shown in Fig. 6 (a) indicates that the height of the peak should not be taken as a measure of expected peak stability. Peaks 2, 4, and 9 are the three most stable peaks, and none of these are the highest peaks. It appears from a qualitative inspection that the narrower peaks are the most stable. The same wavenumber range ( $2\text{cm}^{-1}$ ) is used for all of the figures that appear in Fig. 6 (a) and it is clear there is significant variability in peak stability across the fifteen peaks. The equivalent results are shown for the polymer slide in Fig. 6 (a). In this case peaks 5, 6, and 15 are the three most stable. In general, however, it is clear that the variability of the 4-Acetamidophenol peak positions is approximately half that of the polymer peak positions. The standard deviation of each peak position shown in Fig. 6, is listed in Table 2, as well as the standard deviations for the case of a 1s and 2s acquisition time.

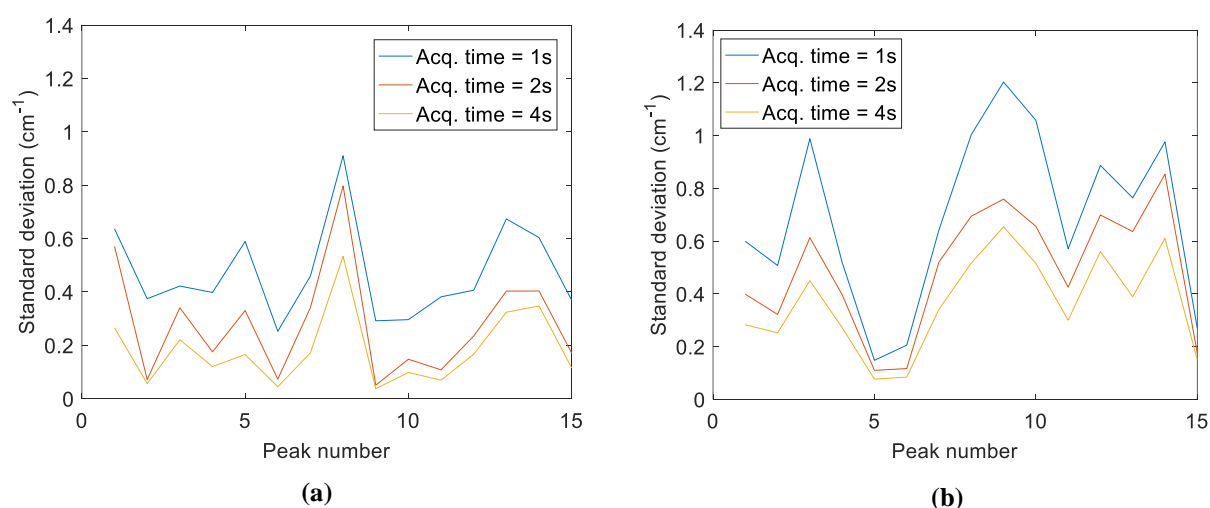


Figure 7. The standard deviation in wavenumber position for each of the fifteen peaks listed in Table 1 for three different acquisition times for (a) 4-Acetamidophenol and (b) the polymer slide.

To provide a visual comparison, the standard deviation of each peak position is represented in graphical format in Fig. 7. Fig.7 (a) shows the standard deviation of all fifteen peaks in the 4-Acetamidophenol spectrum across each dataset of 100 spectra. The three datasets for the 1s, 2s, and 4s acquisition times are shown in different colours in the figure. The range of values is  $(0.25\text{cm}^{-1} - 0.91\text{cm}^{-1})$ ,  $(0.05\text{cm}^{-1} - 0.8\text{cm}^{-1})$ , and  $(0.04\text{cm}^{-1} - 0.53\text{cm}^{-1})$  for the 1s, 2s, and 4s datasets, respectively. As the acquisition time increases, the SNR increases with a square root relationship to time, and it can, therefore, be expected that there will be a related improvement in peak stability; the mean standard deviation of the peak position for the 4s case is  $0.1824\text{cm}^{-1}$ , which is 0.64 times the mean standard deviation for the 2s case, and 0.38 times the standard deviation for the 1s case. A similar trend can be seen for the polymer slide; Fig.7 (b) shows the standard deviation of all fifteen peaks in the polymer spectrum across each dataset of 100 spectra. The range of values is  $(0.21\text{cm}^{-1} - 1.20\text{cm}^{-1})$ ,  $(0.11\text{cm}^{-1} - 0.85\text{cm}^{-1})$ , and  $(0.08\text{cm}^{-1} - 0.61\text{cm}^{-1})$  for the 1s, 2s, and 4s datasets, respectively, which are similar to the values for 4-Acetamidophenol. A reduction in standard deviation is again observed for increased acquisition time; the mean standard deviation of peak position for the 4s case is  $0.36\text{cm}^{-1}$ , which is 0.73 times the mean standard deviation for the 2s case, and 0.52 times the standard deviation for the 1s case. The mean values of the standard deviation of the peaks in the polymer spectrum are approximately double the corresponding values for 4-Acetamidophenol for the 2s and 4s case.

## 5. DISCUSSION

In this paper, we propose a novel wavenumber reference for the calibration of Raman spectra. This material has a number of advantages over existing wavenumber reference materials. These slides are commercially available for life science applications and are manufactured to the same specification as a common glass slide used in microscopy. As such, the slides are ideal for placement on a microscope translation stage. Traditional reference materials are usually associated with health hazards and must be handled with care, and housed in sealed containers that use a window made of glass or a crystal that produces little Raman scattering, such as quartz or Calcium Fluoride. The polymer reference material proposed here can be used without any of these considerations. The slide is inexpensive ( $<€10$ ) and is chemically stable over time, unlike chemicals such as 4-Acetamidophenol, which will inevitably oxidise over an extended duration. The polymer slide appears to be robust to focused laser light and no melting was observed during our experiments using 150mW of a 532nm laser focused using a 10x/0.3 magnification objective. Melting was observed, however, using a 100x/0.9 magnification but stopped with a 50% reduction in laser power. It should be noted that a melting polymer material can irreparably damage the surface of a microscope objective, and care should be taken in this regard.

In Section 2 the various sources of error associated with miscalibration of a Raman spectrum were examined using a series of simulations. Specifically, we investigated an error in grating angle, lateral and rotational camera displacement, and laser wavelength instability. The impact of these errors on the wavenumber axis of a Raman spectrum was simulated using the diffraction grating equation and a simulation of the optical system within a Czerny-Turner spectrograph. It was clear that even small errors can lead to errors in the wavenumber axis of up to  $100\text{cm}^{-1}$ . Analysis of a Raman peak that was analysed over the course of 1000 recordings over a time period of approximately 3 hours, revealed a movement of the peak by almost  $2\text{cm}^{-1}$  due which could result from a small change in ambient room temperature. It can be concluded that temperature control must be applied and frequent wavenumber calibration must be performed throughout daily experiments.

In Section 3 the protocol for calibration of a Raman spectrum using a wavenumber reference was discussed in detail and the position of the fifteen most prominent peaks in the polymer spectrum was found following wavenumber calibration with 4-Acetamidophenol, a commonly used reference material, the Raman spectrum of which contains numerous sharp peaks throughout the fingerprint region. This calibration protocol includes a step to identify the pixel position of given peak with sub-pixel accuracy using spline interpolation. The intensity of the polymer spectrum was found to be approximately the same as the intensity of the 4-Acetamidophenol spectrum, which indicates that similar acquisition times could be used for the polymer material if it is used a reference. The results in Section 4 indicate that on average the stability of the peak positions in the polymer spectrum is approximately half that of the peaks in the 4-Acetamidophenol spectrum; for a 4s acquisition the mean standard deviation of peak position is  $0.18\text{cm}^{-1}$  for 4-Acetamidophenol and  $0.36\text{cm}^{-1}$  for the polymer slide. Based on trends of peak stability for different signal to noise ratios, it can be concluded that these values will reduce significantly for a longer acquisition time, for example 20s. It was not possible to conduct the stability experiment in Section 4 for longer acquisition times because of temperature variability.

The accuracy of the wavenumber calibration protocol that is used in Section 3 could be questioned due to the limited wavenumber resolution of the peak positions in the 4-Acetamidophenol spectrum that were provided by ASTM. These peak positions are accurate to only  $0.1\text{cm}^{-1}$  and it can be expected that a more accurate calibration of the polymer spectrum could be obtained given a more accurate set of peak positions for the reference material that is used to calibrate the polymer spectrum. Furthermore, the spectrograph used in these experiments had a resolution of  $2.5\text{cm}^{-1}$  in the centre of the spectrum, and this increases towards the ends of the spectrum. It can be expected that more accurate results could be obtained using a spectrograph with better resolution.

A final point of note is the limited range over which the peaks in the polymer spectrum are distributed. The peaks that can be used in the wavenumber calibration protocol are distributed over a range from  $743\text{cm}^{-1}$ - $1450\text{cm}^{-1}$  while the 4-Acetamidophenol spectrum contains peaks over a range  $400\text{cm}^{-1}$ - $1650\text{cm}^{-1}$ . We have found that the fit of the polynomial that is returned by the calibration protocol is less accurate outside of the left most and right most available peaks in the reference spectrum. Therefore, it may be expected that the wavenumber axis that is calibrated using the polymer reference would only be accurate within the range just mentioned. This may place a limit on the applicability of this material unless an improved protocol can be developed.

### ACKNOWLEDGMENTS

This research was conducted with the financial support of Science Foundation Ireland (SFI) under Grant number 15/CDA/3667.

### REFERENCES

- [1] Long, Derek Albert, and D. A. Long. Raman spectroscopy. Vol. 206. New York: McGraw-Hill, 1977.
- [2] Santillán, Javier D., Christopher D. Brown, and Wayne Jalenak. "Advances in Raman spectroscopy for explosive identification in aviation security." *Optics and Photonics in Global Homeland Security III*. Vol. 6540. International Society for Optics and Photonics, 2007
- [3] Ellis, David I., and Royston Goodacre. "Metabolic fingerprinting in disease diagnosis: biomedical applications of infrared and Raman spectroscopy." *Analyst* 131.8 (2006): 875-885
- [4] Diem, Max, et al. "Molecular pathology via IR and Raman spectral imaging." *Journal of biophotonics* 6.11-12 (2013): 855-886
- [5] Clemens, Graeme, et al. "Vibrational spectroscopic methods for cytology and cellular research." *Analyst* 139.18 (2014): 4411-4444
- [6] Kerr, L. T., and B. M. Hennelly. "A multivariate statistical investigation of background subtraction algorithms for Raman spectra of cytology samples recorded on glass slides." *Chemometrics and Intelligent Laboratory Systems* 158 (2016): 61-68
- [7] Kerr, Laura T., Hugh J. Byrne, and Bryan M. Hennelly. "Optimal choice of sample substrate and laser wavelength for Raman spectroscopic analysis of biological specimen." *Analytical Methods* 7.12 (2015): 5041-5052
- [8] Kerr, Laura T., et al. "Applications of Raman spectroscopy to the urinary bladder for cancer diagnostics." *Photonics & Lasers in Medicine* 3.3 (2014): 193-224
- [9] Kerr, Laura T., et al. "Methodologies for bladder cancer detection with Raman based urine cytology." *Analytical Methods* 8.25 (2016): 4991-5000
- [10] Crow, P., et al. "The use of Raman spectroscopy to identify and characterize transitional cell carcinoma in vitro." *BJU international* 93.9 (2004): 1232-1236.
- [11] Lyng, Fiona M., et al. "Vibrational spectroscopy for cervical cancer pathology, from biochemical analysis to diagnostic tool." *Experimental and molecular pathology* 82.2 (2007): 121-129
- [12] Carvalho, Luis Felipe CS, et al. "Raman micro-spectroscopy for rapid screening of oral squamous cell carcinoma." *Experimental and molecular pathology* 98.3 (2015): 502-509.
- [13] Jermyn, Michael, et al. "Intraoperative brain cancer detection with Raman spectroscopy in humans." *Science translational medicine* 7.274 (2015): 274ra19-274ra19
- [14] Bergholt, Mads Sylvest, et al. "Fiber-optic Raman spectroscopy probes gastric carcinogenesis in vivo at

- endoscopy." *Journal of biophotonics* 6.1 (2013): 49-59
- [15] Shim, Martin G., et al. "In vivo Near-infrared Raman Spectroscopy: Demonstration of Feasibility During Clinical Gastrointestinal Endoscopy." *Photochemistry and photobiology* 72.1 (2000): 146-150
- [16] Hutsebaut, D. et al. "Evaluation of an accurate calibration and spectral standardization procedure for Raman spectroscopy." *Analyst* 130.8 (2005): 1204-1214
- [17] Rodriguez, Jason D., et al. "Standardization of Raman spectra for transfer of spectral libraries across different instruments." *Analyst* 136.20 (2011): 4232-4240
- [18] Dörfer, Thomas, et al. "Checking and improving calibration of Raman spectra using chemometric approaches." *Zeitschrift für Physikalische Chemie* 225.6-7 (2011): 753-764
- [19] Bocklitz, T. W., et al. "Spectrometer calibration protocol for Raman spectra recorded with different excitation wavelengths." *Spectrochimica Acta Part A: Molecular and Biomolecular Spectroscopy* 149 (2015): 544-549
- [20] Chen, Hui, et al. "Automatic standardization method for Raman spectrometers with applications to pharmaceuticals." *Journal of Raman Spectroscopy* 46.1 (2015): 147-154
- [21] Carrabba, Michael M. "Wavenumber standards for Raman spectrometry." *Handbook of vibrational spectroscopy* (2006).
- [22] Wollman, S. T., and P. W. Bohn. "Evaluation of polynomial fitting functions for use with CCD arrays in Raman spectroscopy." *Applied Spectroscopy* 47.1 (1993): 125-126
- [23] Jones, R. Norman, and A. Nadeau. "Further observations on the use of indene for the wavenumber calibration of infrared spectrometers." *Spectrochimica Acta* 20.7 (1964): 1175-1183
- [24] Berg, Rolf W., and Thomas Nørbygaard. "Wavenumber calibration of CCD detector Raman spectrometers controlled by a sinus arm drive." *Applied Spectroscopy Reviews* 41.2 (2006): 165-183
- [25] Fountain III, Augustus W., Charles K. Mann, and Thomas J. Vickers. "Routine wavenumber calibration of an FT-Raman spectrometer." *Applied spectroscopy* 49.7 (1995): 1048-1053
- [26] Tseng, Ching-Hui, et al. "Wavelength calibration of a multichannel spectrometer." *Applied spectroscopy* 47.11 (1993): 1808-1813
- [27] Skinner, J-G., and W. G. Nilsen. "Absolute Raman scattering cross-section measurement of the 992 cm<sup>-1</sup> line of benzene." *JOSA* 58.1 (1968): 113-119
- [28] Hendra, P. J., and E-J\_ Loader. "Laser Raman spectra of adsorbed species." *Transactions of the Faraday Society* 67 (1971): 828-840
- [29] <https://ibidi.com/content/28-m-slides-and-m-dishes#c374>
- [30] Halidi, Nadia, et al. "Propagation of fast and slow intercellular Ca<sup>2+</sup> waves in primary cultured arterial smooth muscle cells." *Cell calcium* 50.5 (2011): 459-467
- [31] Bessa, Lucinda J., et al. "Synergistic and antibiofilm properties of ocellatin peptides against multidrug-resistant *Pseudomonas aeruginosa*." *Future microbiology* 0 (2018)
- [29] De Boor, Carl, et al. *A practical guide to splines*. Vol. 27. New York: Springer-Verlag, 1978
- [30] Dussault, David, and Paul Hoess. "Noise performance comparison of ICCD with CCD and EMCCD cameras." *Infrared Systems and Photoelectronic Technology*. Vol. 5563. International Society for Optics and Photonics, 2004